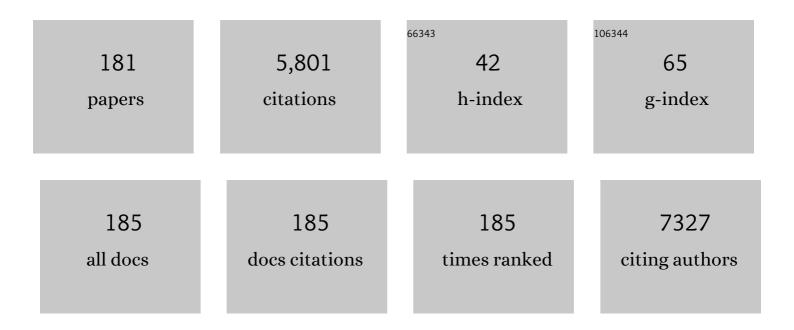
## Michael Wark

List of Publications by Year in descending order

Source: https://exaly.com/author-pdf/6570650/publications.pdf Version: 2024-02-01



#	Article	IF	CITATIONS
1	Mixed metal oxides as efficient electrocatalysts for water oxidation. International Journal of Hydrogen Energy, 2022, 47, 5250-5259.	7.1	14
2	Combinatorial Screening of Cu–W Oxide-Based Photoanodes for Photoelectrochemical Water Splitting. ACS Applied Materials & Interfaces, 2022, 14, 6590-6603.	8.0	6
3	Photocatalytic activity of CoFe2O4/g-C3N4 nanocomposite toward degradation of different organic pollutants and their inactivity toward hydrogen production: The role of the conduction band position. FlatChem, 2022, 32, 100337.	5.6	62
4	Construction of SnO2/g-C3N4 composite photocatalyst with enhanced interfacial charge separation and high efficiency for hydrogen production and Rhodamine B degradation. Colloids and Surfaces A: Physicochemical and Engineering Aspects, 2022, 638, 128288.	4.7	34
5	Reduction of platinum loading in gas diffusion electrodes for high temperature proton exchange membrane fuel cell application: Characterization and effect on oxygen reduction reaction performance. Journal of Power Sources, 2022, 529, 231276.	7.8	9
6	Proton Conductivity of Porous Zirconiumâ€Organic Frameworks Filled with Protic Ionic Liquid. Chemie-Ingenieur-Technik, 2022, 94, 128-134.	0.8	0
7	Impact of the Relative Humidity on the Performance Stability of Anion Exchange Membrane Fuel Cells Studied by Ion Chromatography. ACS Applied Polymer Materials, 2022, 4, 3962-3970.	4.4	7
8	Implementation of different Fe–N–C catalysts in high temperature proton exchange membrane fuel cells – Effect of catalyst and catalyst layer on performance. Journal of Power Sources, 2022, 537, 231529.	7.8	14
9	Discrete Arsonate-Grafted Inverted-Keggin 12-Molybdate Ion [Mo <sub>12</sub> O <sub>32</sub> (OH) <sub>2</sub> (4-N <sub>3</sub> C <sub>2</sub> H <sub>2</sub> -C and Formation of a Copper(II)-Mediated Metal–Organic Framework. Inorganic Chemistry, 2022, , .	< sub <b>4.6</b> <td>b&gt;kd<sub>4<!--</td--></sub></td>	b>kd <sub>4<!--</td--></sub>
10	Discovery and Supramolecular Interactions of Neutral Palladiumâ€Oxo Clusters Pd 16 and Pd 24. Angewandte Chemie, 2021, 133, 3676-3683.	2.0	9
11	Discovery and Supramolecular Interactions of Neutral Palladiumâ€Oxo Clusters Pd <sub>16</sub> and Pd <sub>24</sub> . Angewandte Chemie - International Edition, 2021, 60, 3632-3639.	13.8	24
12	<i>In Situ</i> Synthesis of Co <sub>3</sub> O <sub>4</sub> /CoFe <sub>2</sub> O <sub>4</sub> Derived from a Metal–Organic Framework on Nickel Foam: High-Performance Electrocatalyst for Water Oxidation. ACS Applied Energy Materials, 2021, 4, 2951-2959.	5.1	34
13	Incorporation of Activated Biomasses in Fe-N-C Catalysts for Oxygen Reduction Reaction with Enhanced Stability in Acidic Media. ACS Applied Energy Materials, 2021, 4, 6912-6922.	5.1	15
14	Elucidating Synergistic Effects of Different Metal Ratios in Bimetallic Fe/Co-N-C Catalysts for Oxygen Reduction Reaction. Catalysts, 2021, 11, 841.	3.5	10
15	Chemical Vapor Deposition of Cobalt and Nickel Ferrite Thin Films: Investigation of Structure and Pseudocapacitive Properties. Advanced Materials Interfaces, 2021, 8, 2100949.	3.7	6
16	The Power of Ionic Liquids: Crystal Facet Engineering of SrTiO <sub>3</sub> Nanoparticles for Tailored Photocatalytic Applications. Advanced Sustainable Systems, 2021, 5, 2000180.	5.3	10
17	Relevant Properties of Carbon Support Materials in Successful Fe-N-C Synthesis for the Oxygen Reduction Reaction: Study of Carbon Blacks and Biomass-Based Carbons. Materials, 2021, 14, 45.	2.9	12
18	Discovery of a Neutral 40-Pd <sup>II</sup> -Oxo Molecular Disk, [Pd <sub>40</sub> O <sub>24</sub> (OH) <sub>16</sub> {(CH <sub>3</sub> ) <sub>2</sub> AsO <sub>2</sub> Synthesis, Structural Characterization, and Catabric Studies, Inorganic Chemistry, 2021, 60	>} <sub>16&lt;</sub>	:/sub>]:

18 [Pd<sub>40</sub>0<sub>24</sub>(OH)<sub>16</sub>{(CH<sub>3</sub>)<sub>2</sub>AsO<sub>2</sub>}(sub>}(sub>)<fu) for the sub>16</sub>}: Synthesis, Structural Characterization, and Catalytic Studies. Inorganic Chemistry, 2021, 60, 17339-17347.

#	Article	IF	CITATIONS
19	Enhanced Breaking of Lignin and Mesopore Formation in Zinc Chloride Assisted Hydrothermal Carbonization of Waste Biomasses. Journal of Carbon Research, 2021, 7, 77.	2.7	1
20	Visible light-induced degradation of antibiotic ciprofloxacin over Fe–N–TiO2 mesoporous photocatalyst with anatase/rutile/brookite nanocrystal mixture. Journal of Photochemistry and Photobiology A: Chemistry, 2020, 391, 112371.	3.9	41
21	Photoelectrochemistry of Ferrites: Theoretical Predictions vs. Experimental Results. Zeitschrift Fur Physikalische Chemie, 2020, 234, 719-776.	2.8	24
22	Analysis of the regeneration behavior of high temperature polymer electrolyte membrane fuel cells after hydrogen starvation. Journal of Power Sources, 2020, 449, 227562.	7.8	14
23	Polyoxopalladate-Loaded Metal–Organic Framework (POP@MOF): Synthesis and Heterogeneous Catalysis. Inorganic Chemistry, 2020, 59, 10512-10521.	4.0	23
24	Morphology and Conductivity of Copper Hexacyanoferrate Films. Journal of Physical Chemistry C, 2020, 124, 16849-16859.	3.1	14
25	Semiconductive microporous hydrogen-bonded organophosphonic acid frameworks. Nature Communications, 2020, 11, 3180.	12.8	50
26	Toward developing accelerated stress tests for proton exchange membrane electrolyzers. Current Opinion in Electrochemistry, 2020, 21, 225-233.	4.8	50
27	Tuning Coordination Geometry of Nickel Ketoiminates and Its Influence on Thermal Characteristics for Chemical Vapor Deposition of Nanostructured NiO Electrocatalysts. Inorganic Chemistry, 2020, 59, 10059-10070.	4.0	14
28	Study of Polarization Characteristics of Corrosion Films on Magnesium in Sulfate-Containing Electrolytes. Applied Sciences (Switzerland), 2020, 10, 1406.	2.5	3
29	Machine learning–based optimization for hydrogen purification performance of layered bed pressure swing adsorption. International Journal of Energy Research, 2020, 44, 4475-4492.	4.5	42
30	(Invited) Morphology and Conductivity of Copper Hexacyanoferrate Films. ECS Meeting Abstracts, 2020, MA2020-01, 2810-2810.	0.0	0
31	Hydrothermal Carbonizationâ€Derived Carbon from Waste Biomass as Renewable Pt Support for Fuel Cell Applications: Role of Carbon Activation. Energy Technology, 2019, 7, 1900344.	3.8	20
32	Sequentially Deposited Compact and Pinhole-Free Perovskite Layers via Adjusting the Permittivity of the Conversion Solution. Zeitschrift Fur Naturforschung - Section A Journal of Physical Sciences, 2019, 74, 655-663.	1.5	3
33	Multi-Layered Mesoporous TiO2 Thin Films: Photoelectrodes with Improved Activity and Stability. Coatings, 2019, 9, 625.	2.6	6
34	Zirconium doped mesoporous TiO2 multilayer thin films: Influence of the zirconium content on the photodegradation of organic pollutants. Catalysis Today, 2019, 328, 71-78.	4.4	23
35	Discovery of Polyoxo-Noble-Metalate-Based Metal–Organic Frameworks. Journal of the American Chemical Society, 2019, 141, 3385-3389.	13.7	43
36	Excellent photocatalytic reduction of nitroarenes to aminoarenes by BiVO <sub>4</sub> nanoparticles grafted on reduced graphene oxide (rGO/BiVO <sub>4</sub> ). Applied Organometallic Chemistry, 2019, 33, e5059.	3.5	19

#	Article	IF	CITATIONS
37	Characterization methodology for anode starvation in HT-PEM fuel cells. International Journal of Hydrogen Energy, 2019, 44, 18330-18339.	7.1	11
38	Sol–gel chemistry in molten BrÃ,nsted acids towards "activated―carbons and beyond. Nanoscale, 2019, 11, 13154-13160.	5.6	3
39	Perovskite-type LaFeO3: Photoelectrochemical Properties and Photocatalytic Degradation of Organic Pollutants Under Visible Light Irradiation. Catalysts, 2019, 9, 342.	3.5	110
40	Co-composted hydrochar substrates as growing media for horticultural crops. Scientia Horticulturae, 2019, 252, 96-103.	3.6	28
41	Graphitic carbon nitride synthesized by simple pyrolysis: role of precursor in photocatalytic hydrogen production. New Journal of Chemistry, 2019, 43, 6909-6920.	2.8	116
42	Photocatalytic activity of ZrO <sub>2</sub> composites with graphitic carbon nitride for hydrogen production under visible light. New Journal of Chemistry, 2019, 43, 4455-4462.	2.8	101
43	Micro-spectroscopy of HKUST-1 metal–organic framework crystals loaded with tetracyanoquinodimethane: effects of water on host–guest chemistry and electrical conductivity. Physical Chemistry Chemical Physics, 2019, 21, 25678-25689.	2.8	15
44	The Effect of Donor Additives on the Stability and Structure of 5â€Diphenylphosphinoacenaphthâ€6â€yllithium. European Journal of Inorganic Chemistry, 2019, 2019, 712-720.	2.0	8
45	Construction of strontium tantalate homo-semiconductor composite photocatalysts with a tunable type II junction structure for overall water splitting. Catalysis Science and Technology, 2018, 8, 3025-3033.	4.1	8
46	Prediction of delamination state of 2D filler materials in cyclic olefin copolymer for enhanced barrier applications. Composite Structures, 2018, 202, 853-859.	5.8	3
47	Rational Development of Cobalt β-Ketoiminate Complexes: Alternative Precursors for Vapor-Phase Deposition of Spinel Cobalt Oxide Photoelectrodes. Inorganic Chemistry, 2018, 57, 5133-5144.	4.0	14
48	Layered cesium copper titanate for photocatalytic hydrogen production. Applied Catalysis B: Environmental, 2018, 227, 349-355.	20.2	23
49	Solid state route for synthesis of YFeO3/g-C3N4 composites and its visible light activity for degradation of organic pollutants. Catalysis Today, 2018, 313, 47-54.	4.4	55
50	Organic Cation Substitution in Hybrid Perovskite CH <sub>3</sub> NH <sub>3</sub> PbI <sub>3</sub> with Hydroxylammonium (NH <sub>3</sub> OH <sup>+</sup> ): A First-Principles Study. Journal of Physical Chemistry C, 2018, 122, 3548-3557.	3.1	13
51	Photocatalytic degradation of the herbicide chloridazon on mesoporous titania/zirconia nanopowders. Environmental Science and Pollution Research, 2018, 25, 34873-34883.	5.3	16
52	Microwave assisted synthesis of Ta2O5 nanostructures for photocatalytic hydrogen production. Journal of Photochemistry and Photobiology A: Chemistry, 2018, 366, 41-47.	3.9	14
53	Proton mobility in sulfonic acid functionalized mesoporous materials studied by MAS PFG NMR diffusometry and impedance spectroscopy. Microporous and Mesoporous Materials, 2018, 255, 140-147.	4.4	11
54	Combinatorial screening of photoanode materials - Uniform platform for compositional arrays and macroscopic electrodes. Electrochimica Acta, 2018, 259, 204-212.	5.2	12

#	Article	IF	CITATIONS
55	Green Synthesis of a New Alâ€MOF Based on the Aliphatic Linker Mesaconic Acid: Structure, Properties and In Situ Crystallisation Studies of Alâ€MILâ€68â€Mes. Chemistry - A European Journal, 2018, 24, 2173-2181.	3.3	33
56	Crystalline and permanently porous porphyrin-based metal tetraphosphonates. Chemical Communications, 2018, 54, 389-392.	4.1	52
57	Reprint of "Photoelectrocatalytic behavior of electrodeposited zinc ferrite films with varying Zn:Fe ratio― Journal of Photochemistry and Photobiology A: Chemistry, 2018, 366, 18-26.	3.9	1
58	Photoelectrocatalytic behavior of electrodeposited zinc ferrite films with varying Zn:Fe ratio. Journal of Photochemistry and Photobiology A: Chemistry, 2018, 362, 49-57.	3.9	8
59	Recent Progress in the Solution-Based Sequential Deposition of Planar Perovskite Solar Cells. Crystal Growth and Design, 2018, 18, 4790-4806.	3.0	12
60	Scale-Up of the Electrodeposition of ZnO/Eosin Y Hybrid Thin Films for the Fabrication of Flexible Dye-Sensitized Solar Cell Modules. Materials, 2018, 11, 232.	2.9	23
61	Durability of Electrocatalysts for ORR: Pt on Nanocomposite of Reduced Graphene Oxide with FTO versus Pt/C. Journal of the Electrochemical Society, 2018, 165, F3373-F3382.	2.9	30
62	Photoactive Zinc Ferrites Fabricated via Conventional CVD Approach. ACS Sustainable Chemistry and Engineering, 2017, 5, 2917-2926.	6.7	41
63	Formation of hybrid ABX <sub>3</sub> perovskite compounds for solar cell application: first-principles calculations of effective ionic radii and determination of tolerance factors. Dalton Transactions, 2017, 46, 3500-3509.	3.3	133
64	Stability of Pt Nanoparticles on Alternative Carbon Supports for Oxygen Reduction Reaction. Journal of the Electrochemical Society, 2017, 164, F995-F1004.	2.9	59
65	Investigation of Reduced Graphene Oxide with F-Doped SnO2as Catalyst Support in Fuel Cells. ECS Transactions, 2017, 80, 879-895.	0.5	2
66	Rational fabrication of a graphitic-C <sub>3</sub> N <sub>4</sub> /Sr <sub>2</sub> KNb <sub>5</sub> O <sub>15</sub> nanorod composite with enhanced visible-light photoactivity for degradation of methylene blue and hydrogen production. RSC Advances, 2017, 7, 42774-42782.	3.6	4
67	Lithium Insertion into Mixed Phase Titania Nanotubes. Zeitschrift Fur Physikalische Chemie, 2017, 231, 1407-1421.	2.8	2
68	Microwave-Assisted Synthesis of Perovskite SrSnO <sub>3</sub> Nanocrystals in Ionic Liquids for Photocatalytic Applications. Inorganic Chemistry, 2017, 56, 6920-6932.	4.0	62
69	Synthesis of Phase Pure Hexagonal YFeO3 Perovskite as Efficient Visible Light Active Photocatalyst. Catalysts, 2017, 7, 326.	3.5	53
70	Challenges in Automotive Fuel Cells Recycling. Recycling, 2016, 1, 343-364.	5.0	35
71	Photoactivity and scattering behavior of anodically and cathodically deposited hematite photoanodes – a comparison by scanning photoelectrochemical microscopy. Electrochimica Acta, 2016, 202, 224-230.	5.2	12
72	Adsorption - wenn Ingenieure und Chemiker sich treffen …. Chemie-Ingenieur-Technik, 2016, 88, 223-223.	0.8	0

#	Article	IF	CITATIONS
73	Proton Conduction in Sulfonated Organic–Inorganic Hybrid Monoliths with Hierarchical Pore Structure. ACS Applied Materials & Interfaces, 2016, 8, 25476-25488.	8.0	12
74	Photoelectrochemical and theoretical investigations of spinel type ferrites (M <sub><i>x</i></sub> Fe <sub>3â^'<i>x</i></sub> O <sub>4</sub> ) for water splitting: a mini-review. Journal of Photonics for Energy, 2016, 7, 012009.	1.3	111
75	Improved charge carrier separation in barium tantalate composites investigated by laser flash photolysis. Physical Chemistry Chemical Physics, 2016, 18, 10719-10726.	2.8	25
76	Hydrothermal carbonization of biomass from landscape management – Influence of process parameters on soil properties of hydrochars. Journal of Environmental Management, 2016, 173, 72-78.	7.8	34
77	Cr <sub>2</sub> O <sub>3</sub> Nanoparticles on Ba <sub>5</sub> Ta <sub>4</sub> O <sub>15</sub> as a Nobleâ€Metalâ€Free Oxygen Evolution Co atalyst for Photocatalytic Overall Water Splitting. ChemCatChem, 2016, 8, 153-156.	3.7	34
78	Research Update: Photoelectrochemical water splitting and photocatalytic hydrogen production using ferrites (MFe2O4) under visible light irradiation. APL Materials, 2015, 3, .	5.1	92
79	Three Series of Sulfoâ€Functionalized Mixedâ€Linker CAUâ€10 Analogues: Sorption Properties, Proton Conductivity, and Catalytic Activity. Chemistry - A European Journal, 2015, 21, 12517-12524.	3.3	49
80	Theoretical and Experimental Study of Anatase Nanotube Formation via Sodium Titanate Intermediates. Journal of Physical Chemistry C, 2015, 119, 5048-5054.	3.1	6
81	CNT-TiO2â <sup>~^</sup> δ Composites for Improved Co-Catalyst Dispersion and Stabilized Photocatalytic Hydrogen Production. Catalysts, 2015, 5, 270-285.	3.5	18
82	Correlating Changes in Electron Lifetime and Mobility on Photocatalytic Activity at Network-Modified TiO <sub>2</sub> Aerogels. Journal of Physical Chemistry C, 2015, 119, 17529-17538.	3.1	42
83	Active Sites for Light Driven Proton Reduction in Y2Ti2O7 and CsTaWO6 Pyrochlore Catalysts Detected by In Situ EPR. Topics in Catalysis, 2015, 58, 769-775.	2.8	9
84	New insight into calcium tantalate nanocomposite photocatalysts for overall water splitting and reforming of alcohols and biomass derivatives. APL Materials, 2015, 3, 104412.	5.1	8
85	Electrochemical deposition of Fe <sub>2</sub> O <sub>3</sub> in the presence of organic additives: a route to enhanced photoactivity. RSC Advances, 2015, 5, 103512-103522.	3.6	34
86	Understanding the Influence of Lattice Composition on the Photocatalytic Activity of Defectâ€Pyrochlore‧tructured Semiconductor Mixed Oxides. Advanced Functional Materials, 2015, 25, 905-912.	14.9	26
87	Low-temperature route to metal titanate perovskite nanoparticles for photocatalytic applications. Applied Catalysis B: Environmental, 2015, 178, 20-28.	20.2	74
88	Limits of ZnO Electrodeposition in Mesoporous Tin Doped Indium Oxide Films in View of Application in Dye-Sensitized Solar Cells. Materials, 2014, 7, 3291-3304.	2.9	4
89	Photocatalytic hydrogen production with non-stoichiometric pyrochlore bismuth titanate. Catalysis Today, 2014, 225, 102-110.	4.4	47
90	Phosphonic acid anchored ruthenium complexes for ZnO-based dye-sensitized solar cells. Dyes and Pigments, 2014, 104, 24-33.	3.7	26

#	Article	IF	CITATIONS
91	Improved overall water splitting with barium tantalate mixed oxide composites. Chemical Science, 2014, 5, 3746-3752.	7.4	49
92	Tetragonal tungsten bronze-type nanorod photocatalysts with tunnel structures: Ta substitution for Nb and overall water splitting. Journal of Materials Chemistry A, 2014, 2, 8815-8822.	10.3	33
93	Sol–gel synthesis of defect-pyrochlore structured CsTaWO6 and the tribochemical influences on photocatalytic activity. RSC Advances, 2013, 3, 18908.	3.6	34
94	Carbon blacks for the extension of the cycle life in flooded lead acid batteries forÂmicro-hybrid applications. Journal of Power Sources, 2013, 239, 483-489.	7.8	59
95	Bimodal mesoporous titanium dioxide anatase films templated by a block polymer and an ionic liquid: influence of the porosity on the permeability. Nanoscale, 2013, 5, 12316.	5.6	24
96	High-throughput microwave-assisted discovery of new metal phosphonates. Dalton Transactions, 2013, 42, 8761.	3.3	20
97	Carbon blacks for lead-acid batteries in micro-hybrid applications – Studied by transmission electron microscopy and Raman spectroscopy. Journal of Power Sources, 2013, 222, 554-560.	7.8	47
98	Electrodeposition of zinc oxide on transparent conducting metal oxide nanofibers and its performance in dye sensitized solar cells. Electrochimica Acta, 2013, 90, 375-381.	5.2	37
99	A carbon nanotube-based transparent conductive substrate for flexible ZnO dye-sensitized solar cells. Thin Solid Films, 2013, 531, 391-397.	1.8	16
100	Control of Phase Coexistence in Calcium Tantalate Composite Photocatalysts for Highly Efficient Hydrogen Production. Chemistry of Materials, 2013, 25, 4739-4745.	6.7	41
101	Enhanced photocatalytic hydrogen generation from barium tantalate composites. Photochemical and Photobiological Sciences, 2013, 12, 671-677. Effects of Nonstoichiometry and Cocatalyst Loading on the Photocatalytic Hydrogen Production	2.9	57
102	with ( <scp><scp>Y</scp></scp> <sub>1.5</sub> <scp>Si</scp> <sub>0.5</sub> ) <sub>1â^'<i>x</i>and</sub>	0.0	/
103	<pre>(<scp><scp>YBi</scp></scp>)<sub>1â<sup>°</sup><i>x</i></sub><scp><scp>Ti</scp></scp><sub>2</sub><scp>C&lt; Pyrochlores. Journal of the American Ceramic Society, 2013, 96, 634-642. Influence of Coumarin 343 Monomer Codeposition on the Structure and Electronic Properties of Electrodeposited ZnO. Journal of Physical Chemistry C, 2012, 116, 5610-5613.</scp></pre>	3.1	o> <sub>7a :</sub>
104	Distribution of functional groups in periodic mesoporous organosilica materials studied by small-angle neutron scattering with in situ adsorption of nitrogen. Beilstein Journal of Nanotechnology, 2012, 3, 428-437.	2.8	6
105	Investigation of the pulsed electrochemical deposition of ZnO. Electrochimica Acta, 2012, 80, 60-67.	5.2	8
106	Electrodeposited Prussian Blue in mesoporous TiO2 as electrochromic hybrid material. Microporous and Mesoporous Materials, 2012, 164, 67-70.	4.4	29
107	Proton transport in functionalised additives for PEM fuel cells: contributions from atomistic simulations. Chemical Society Reviews, 2012, 41, 5143.	38.1	27
108	Improved Photocatalytic Hydrogen Production by Structure Optimized Nonstoichiometric Y <sub>2</sub> Ti <sub>2</sub> O <sub>7</sub> . ChemCatChem, 2012, 4, 1819-1827.	3.7	26

#	Article	IF	CITATIONS
109	Composite proton-conducting polymer membranes for clean hydrogen production with solar light in a simple photoelectrochemical compartment cell. International Journal of Hydrogen Energy, 2012, 37, 4012-4017.	7.1	27
110	Investigation on the optimal oxidation agent for a maximum yield of sulfonic acid groups in MCM-41. Microporous and Mesoporous Materials, 2012, 151, 506-510.	4.4	9
111	Highly proton conducting sulfonic acid functionalized mesoporous materials studied by impedance spectroscopy, MAS NMR spectroscopy and MAS PFG NMR diffusometry. Microporous and Mesoporous Materials, 2012, 156, 80-89.	4.4	28
112	Multilayered ordered mesoporous platinum/titania composite films: does the photocatalytic activity benefit from the film thickness?. Journal of Materials Chemistry, 2011, 21, 7802.	6.7	37
113	Detection of Homogeneous Distribution of Functional Groups in Mesoporous Silica by Small Angle Neutron Scattering and in Situ Adsorption of Nitrogen or Water. Langmuir, 2011, 27, 5516-5522.	3.5	21
114	pH-Control of the Photocatalytic Degradation Mechanism of Rhodamine B over Pb <sub>3</sub> Nb <sub>4</sub> O <sub>13</sub> . Journal of Physical Chemistry C, 2011, 115, 8014-8023.	3.1	115
115	Low Temperature Preparation of Porous Crystalline TiO2 Films Using a Combination of Electrochemical and Electrophoretical Deposition. Journal of Advanced Oxidation Technologies, 2011, 14, .	0.5	0
116	Solid-state dye-sensitized ZnO solar cells prepared by low-temperature methods. Journal of Applied Electrochemistry, 2011, 41, 445-452.	2.9	13
117	Proton Conductivity of SO <sub>3</sub> Hâ€Functionalized Benzene–Periodic Mesoporous Organosilica. Small, 2011, 7, 1086-1097.	10.0	36
118	Passive Mischelemente zur Elektrolytkonvektion in Blei-SÃ <b>¤</b> re-Nassbatterien. Chemie-Ingenieur-Technik, 2011, 83, 2051-2058.	0.8	15
119	Proton onducting Composite Membranes for Future Perspective Applications in Fuel Cells, Desalination Facilities and Photocatalysis. Chemie-Ingenieur-Technik, 2011, 83, 2177-2187.	0.8	3
120	Investigation of Liquid Additives on the Nano-Hardness of NiFe during Polishing. Tribology Online, 2011, 6, 113-116.	0.9	0
121	Efficiency improvement of dye-sensitized solar cells based on electrodeposited TiO2 films by low temperature post-treatment. Electrochimica Acta, 2010, 55, 6352-6357.	5.2	14
122	Ultra-long SiO2 and SiO2/TiO2 tubes embedded with Pt nanoparticles using magnus green salt as templating structures. Journal of Materials Science, 2010, 45, 1179-1188.	3.7	9
123	Proton conductivity of ordered mesoporous materials containing aluminium. Journal of Power Sources, 2010, 195, 7781-7786.	7.8	8
124	A low-cost procedure for the preparation of mesoporous layers of TiO2 efficient in the environmental clean-up. Journal of Photochemistry and Photobiology A: Chemistry, 2010, 216, 126-132.	3.9	24
125	Molecular and supramolecular templating of silicaâ€based nanotubes and introduction of metal nanowires. Physica Status Solidi (B): Basic Research, 2010, 247, 2401-2411.	1.5	13
126	Palladium Doped Porous Titania Photocatalysts: Impact of Mesoporous Order and Crystallinity. Chemistry of Materials, 2010, 22, 108-116.	6.7	203

#	Article	IF	CITATIONS
127	Pore size and surface charge control in mesoporous TiO2 using post-grafted SAMs. Physical Chemistry Chemical Physics, 2010, 12, 1473.	2.8	25
128	Nanoparticulate Dye-Semiconductor Hybrid Materials Formed by Electrochemical Self-Assembly as Electrodes in Photoelectrochemical Cells. Zeitschrift Fur Naturforschung - Section A Journal of Physical Sciences, 2009, 64, 518-530.	1.5	1
129	Nanoparticles of Mesoporous SO <sub>3</sub> Hâ€Functionalized Siâ€MCMâ€41 with Superior Proton Conductivity. Small, 2009, 5, 854-859.	10.0	54
130	Ion conductivity of nano-scaled Al-rich ZSM-5 synthesized in the pores of carbon black. Microporous and Mesoporous Materials, 2009, 120, 47-52.	4.4	29
131	Proton conductivity of imidazole functionalized ordered mesoporous silica: Influence of type of anchorage, chain length and humidity. Microporous and Mesoporous Materials, 2009, 123, 21-29.	4.4	43
132	Detailed Simulation and Characterization of Highly Proton Conducting Sulfonic Acid Functionalized Mesoporous Materials under Dry and Humidified Conditions. Journal of Physical Chemistry C, 2009, 113, 19218-19227.	3.1	28
133	Improving the Photocatalytic Performance of Mesoporous Titania Films by Modification with Gold Nanostructures. Chemistry of Materials, 2009, 21, 1645-1653.	6.7	170
134	Gold Nanoparticles on Mesoporous Interparticle Networks of Titanium Dioxide Nanocrystals for Enhanced Photonic Efficiencies. Journal of Physical Chemistry C, 2009, 113, 7429-7435.	3.1	193
135	New proton conducting hybrid membranes for HT-PEMFC systems based on polysiloxanes and SO3H-functionalized mesoporous Si-MCM-41 particles. Journal of Membrane Science, 2008, 316, 164-175.	8.2	53
136	Development of polyoxadiazole nanocomposites for high temperature polymer electrolyte membrane fuel cells. Journal of Membrane Science, 2008, 322, 406-415.	8.2	38
137	A comparative study into the photocatalytic properties of thin mesoporous layers of TiO2 with controlled mesoporosity. Journal of Photochemistry and Photobiology A: Chemistry, 2008, 194, 181-188.	3.9	55
138	Highly porous TiO2 films from anodically deposited titanate hybrids and their photoelectrochemical and photocatalytic activity. Microporous and Mesoporous Materials, 2008, 111, 55-61.	4.4	18
139	Influence of Calcination Temperature on the Photoelectrochemical and Photocatalytic Properties of Porous TiO <sub>2</sub> Films Electrodeposited from Ti(IV)-Alkoxide Solution. Journal of Physical Chemistry C, 2008, 112, 15122-15128.	3.1	36
140	ELECTRODEPOSITION OF GOLD STRUCTURES IN MESOPOROUS <font>TIO</font> <sub>2</sub> SOL-GEL FILMS. , 2008, , .		0
141	Functionalized mesoporous materials used as proton conductive additives for high temperature PEM fuel cell membranes. Studies in Surface Science and Catalysis, 2007, 170, 1540-1545.	1.5	3
142	Texture properties of nanoporous TiO2 films prepared by anodic electrodeposition using a structure-directing agent. Studies in Surface Science and Catalysis, 2007, 170, 1494-1501.	1.5	4
143	Ion-Permselective pH-Switchable Mesoporous Silica Thin Layers. Chemistry of Materials, 2007, 19, 1640-1647.	6.7	62
144	Illumination-induced properties of highly ordered mesoporous TiO2 layers with controlled crystallinity. Thin Solid Films, 2007, 515, 6541-6543.	1.8	15

#	Article	IF	CITATIONS
145	SiO2 nanotubes with nanodispersed Pt in the walls. Microporous and Mesoporous Materials, 2007, 99, 30-36.	4.4	14
146	Proton conductivity of sulfonic acid functionalised mesoporous materials. Microporous and Mesoporous Materials, 2007, 99, 190-196.	4.4	84
147	Electrode layers for electrochemical applications based on functionalized mesoporous silica films. Sensors and Actuators B: Chemical, 2007, 126, 78-81.	7.8	15
148	Crystallization of Indium Tin Oxide Nanoparticles: From Cooperative Behavior to Individuality. Small, 2007, 3, 310-317.	10.0	45
149	Microstructure and magnetic properties of tubular cobalt–silica nanocomposites. Journal of Magnetism and Magnetic Materials, 2007, 312, 405-409.	2.3	4
150	Ordered Functionalized Silica Materials with High Proton Conductivity. Chemistry of Materials, 2007, 19, 6401-6407.	6.7	90
151	Low-Temperature Preparation of Crystalline Nanoporous TiO[sub 2] Films by Surfactant-Assisted Anodic Electrodeposition. Electrochemical and Solid-State Letters, 2006, 9, C93.	2.2	37
152	Nonaqueous Synthesis of Uniform Indium Tin Oxide Nanocrystals and Their Electrical Conductivity in Dependence of the Tin Oxide Concentration. Chemistry of Materials, 2006, 18, 2848-2854.	6.7	157
153	Role of the Critical Micelle Concentration in the Electrochemical Deposition of Nanostructured ZnO Films under Utilization of Amphiphilic Molecules. Langmuir, 2006, 22, 9427-9430.	3.5	30
154	Photocatalytic activity of hydrophobized mesoporous thin films of TiO2. Microporous and Mesoporous Materials, 2005, 84, 247-253.	4.4	69
155	Self-integration of aligned cobalt nanoparticles into silica nanotubes. Applied Physics Letters, 2005, 87, 212503.	3.3	6
156	Functionalized Mesoporous Silica Films as a Matrix for Anchoring Electrochemically Active Guests. Langmuir, 2005, 21, 11320-11329.	3.5	102
157	Controlled Growth of Pt-Containing SiO2 Nanotubes with High Aspect Ratios. Chemistry of Materials, 2005, 17, 5928-5934.	6.7	11
158	Homogeneously distributed CdS and CdSe nanoparticles in thin films of mesoporous silica. Thin Solid Films, 2004, 458, 20-25.	1.8	15
159	Title is missing!. Journal of Sol-Gel Science and Technology, 2003, 26, 483-488.	2.4	37
160	Optical gas sensing by semiconductor nanoparticles or organic dye molecules hosted in the pores of mesoporous siliceous MCM-41. Physical Chemistry Chemical Physics, 2003, 5, 5188-5194.	2.8	37
161	SnO2 nanoparticles in the pores of non-structured SiO2 and Si-MCM-41: Comparison of their properties in gas sensing. Studies in Surface Science and Catalysis, 2002, 141, 653-660.	1.5	8
162	Semiconductor nanoparticles in the channels of mesoporous silica and titania thin films. Studies in Surface Science and Catalysis, 2002, 142, 1457-1464.	1.5	3

#	Article	IF	CITATIONS
163	Titanium Oxide Species in Molecular Sieves:Â Materials for the Optical Sensing of Reductive Gas Atmospheres. Chemistry of Materials, 2002, 14, 2458-2466.	6.7	38
164	Anchorage of dye molecules and organic moieties to the inner surface of Si-MCM-41. Studies in Surface Science and Catalysis, 2002, 142, 1067-1074.	1.5	9
165	Metal clusters in plasma polymer matrices. Physical Chemistry Chemical Physics, 2002, 4, 2438-2442.	2.8	13
166	Detection of nanodefects in the framework of NaY zeolite originating from the in situ synthesis of metal-free phthalocyanine. Microporous and Mesoporous Materials, 2002, 56, 131-138.	4.4	6
167	METAL SALTS AS STRUCTURE-DIRECTING AGENTS FOR SIO2 AND TIO2 NANOTUBES CONTAINING HIGH AMOUNTS OF ENCAPSULATED METAL. , 2002, , .		1
168	Microwave-assisted preparation of uniform pure and dye-loaded AlPO4-5 crystals with different morphologies for use as microlaser systems. Journal of Materials Chemistry, 2001, 11, 1823-1827.	6.7	29
169	Photochromism of spiropyran in molecular sieve voids: effects of host–guest interaction on isomer status, switching stability and reversibility. Journal of Materials Chemistry, 2001, 11, 2014-2021.	6.7	65
170	Redox behaviour of SnO2 nanoparticles encapsulated in the pores of zeolites towards reductive gas atmospheres studied by in situ diffuse reflectance UV/Vis and MA¶ssbauer spectroscopy. Physical Chemistry Chemical Physics, 2001, 3, 1870-1876.	2.8	27
171	Anchoring of Functional Dye Molecules in MCM-41 by Microwave-Assisted Hydrothermal Cocondensation. Angewandte Chemie - International Edition, 2000, 39, 160-163.	13.8	92
172	Metallorganic Routes to Nanoscale Iron and Titanium Oxide Particles Encapsulated in Mesoporous Alumina: Formation, Physical Properties, and Chemical Reactivity. Chemistry - A European Journal, 2000, 6, 4305-4321.	3.3	37
173	Covalent attachment of dye molecules to the inner surface of MCM-41. Studies in Surface Science and Catalysis, 2000, 129, 295-302.	1.5	13
174	Metal clusters in plasma polymer matrices. Part III. Optical properties and redox behaviour of Cu clusters. Physical Chemistry Chemical Physics, 2000, 2, 3105-3110.	2.8	19
175	Platinum-filled oxidic nanotubes. Microporous and Mesoporous Materials, 1999, 31, 235-239.	4.4	64
176	Metal clusters in plasma polymer matrices Part II. Silver clusters. Physical Chemistry Chemical Physics, 1999, 1, 4447-4451.	2.8	31
177	Reducibility of vanadium oxide species in MCM-41. Microporous and Mesoporous Materials, 1998, 22, 225-236.	4.4	81
178	Reduction Kinetics of Zeolite-Hosted Mono- and Polynuclear Titanium Oxide Species Followed by UV/Vis Diffuse Reflectance Spectroscopy:  Influence of Location and Coordination. Journal of Physical Chemistry B, 1998, 102, 1665-1671.	2.6	43
179	Cadmium ion exchange in zeolite Y by chemical vapour deposition and reaction. Journal of Materials Chemistry, 1997, 7, 1429-1432.	6.7	17
180	Growth and reactivity of zinc and cadmium oxide nano-particles in zeolites. Microporous Materials, 1997, 8, 241-253.	1.6	41

#	Article	IF	CITATIONS
181	X-ray photoelectron/X-ray excited auger electron spectroscopic study of highly dispersed semiconductor CdS and CdO species in zeolites. Journal of the Chemical Society, Faraday Transactions, 1993, 89, 3987.	1.7	39